Journal of Ginseng Research 47 (2023) 543–551

Contents lists available at ScienceDirect

Journal of Ginseng Research

journal homepage: https://www.sciencedirect.com/journal/journal-of-ginseng-research

Research Article

Ginseng saponin metabolite 20(S)-protopanaxadiol relieves pulmonary fibrosis by multiple-targets signaling pathways

Guoqing Ren [a, b], Weichao Lv [a, b], Yue Ding [a, b], Lei Wang [a, b], ZhengGuo Cui [a, c], Renshi Li [a, b], Jiangwei Tian [a, b, **], Chaofeng Zhang [a, b, *]

[a] Sino-Jan Joint Laboratory of Natural Health Products Research, School of Traditional Chinese Pharmacy, China Pharmaceutical University, Nanjing, China
[b] State Key Laboratory of Natural Medicines, China Pharmaceutical University, Nanjing, China
[c] Department of Environmental Health, University of Fukui School of Medical Science, Fukui, Japan

ARTICLE INFO

Article history:
Received 5 February 2022
Received in revised form
4 December 2022
Accepted 4 January 2023
Available online 7 January 2023

Keywords:
20(S)-protopanaxadiol
Adenosine 5'monophosphate-activated protein kinase
Pulmonary fibrosis
Stimulator of interferon genes

ABSTRACT

Background: Panax ginseng Meyer is a representative Chinese herbal medicine with antioxidant and anti-inflammatory activity. 20(S)-Protopanaxadiol (PPD) has been isolated from ginseng and shown to have promising pharmacological activities. However, effects of PDD on pulmonary fibrosis (PF) have not been reported. We hypothesize that PDD may reverse inflammation-induced PF and be a novel therapeutic strategy.

Methods: Adult male C57BL/6 mice were used to establish a model of PF induced by bleomycin (BLM). The pulmonary index was measured, and histological and immunohistochemical examinations were made. Cell cultures of mouse alveolar epithelial cells were analyzed with Western blotting, co-immunoprecipitation, immunofluorescence, immunohistochemistry, siRNA transfection, cellular thermal shift assay and qRT-PCR.

Results: The survival rate of PPD-treated mice was higher than that of untreated BLM-challenged mice. Expression of fibrotic hallmarks, including α-SMA, TGF-β1 and collagen I, was reduced by PPD treatment, indicating attenuation of PF. Mice exposed to BLM had higher STING levels in lung tissue, and this was reduced by phosphorylated AMPK after activation by PPD. The role of phosphorylated AMPK in suppressing STING was confirmed in TGF-β1-incubated cells. Both *in vivo* and *in vitro* analyses indicated that PPD treatment attenuated BLM-induced PF by modulating the AMPK/STING signaling pathway.

Conclusion: PPD ameliorated BLM-induced PF by multi-target regulation. The current study may help develop new therapeutic strategies for preventing PF.

1. Introduction

The pathogenesis of pulmonary fibrosis (PF) involves complex interactions between multiple cell types and signaling pathways. Damage to alveolar epithelial cells may lead to metabolic dysfunction, aging, abnormal activation of epithelial cells and disordered epithelial repair. Mesenchymal, immune and endothelial cells are modulated through a variety of signaling mechanisms, triggering activation of fibroblasts and myofibroblasts [1,2]. The exact mechanism triggering PF is unclear, but oxidative stress, procoagulant environment, inflammation and immune mechanisms in the lung may be involved [3–8]. Therefore, the relationship between immune function and PF diseases merits research scrutiny.

In recent years, the influence of immunotherapy on the innate immune system and its potential for the treatment of fibrosis has been highlighted [9]. Stimulator of interferon genes (STING) and the innate immune pathway are involved in antiviral defense, and dysregulation may promote cancer or autoimmunity and auto-inflammatory disease [10,11]. STING is thought to be related to lung inflammation and fibrosis [12,13].

Panax ginseng extract is known to invigorate lung tissue and delay PF progression. Jang et al [14] examined changes in

** Corresponding author. Sino-Jan Joint Laboratory of Natural Health Products Research, School of Traditional Chinese Pharmacy, China Pharmaceutical University, Nanjing, 639 Longmian Road, China.
* Corresponding author. Sino-Jan Joint Laboratory of Natural Health Products Research, School of Traditional Chinese Pharmacy, China Pharmaceutical University, Nanjing, 639 Longmian Road, China.
E-mail addresses: jwtian@cpu.edu.cn (J. Tian), zhangchaofeng@cpu.edu.cn (C. Zhang).

https://doi.org/10.1016/j.jgr.2023.01.002

superoxide dismutase and malondialdehyde and found that intragastric administration of high-dose Panax ginseng extract reduced oxidative damage in radiation-induced PF. Renshen Pingfei Decoction is a traditional Chinese herbal formula in which Panax ginseng is the main drug (The ratio of *Panax ginseng* C.A.Mey.: *Asparagus cochinchinensis* (Lour.) Merr.: *Morus alba* L.: *Lycium chinense* Mill.: *Glycyrrhiza uralensis* Fisch.: *Anemarrhena asphodeloides* Bunge: *Citrus reticulata* Blanco in Renshen Pingfei Decoction was 1:1:1:1:1:1:1. The herbs were decocted and concentrated with each milliliter containing 0.65g of crude drugs.). The formula contributed to the amelioration of PF in bleomycin (BLM)-damaged rats. Treated lungs had lower levels of hydroxyproline, a collagen component, indicating reduced collagen synthesis. Panax ginseng was shown to interfere with the TGF-β1/Smad3 signaling pathway [15]. In addition, Bai et al [16] investigated intragastric administration of the Jinshui Huanxian formula (11 medicinal herbs, including Ginseng Radix, Ophiopogonis Radix and Rehmanniae Radix. All herbs were water or ethanol extracted and dried. Each 1 g of dry extract contains 3.13 g of raw herbs). Treatment recovered lung function parameters, such as forced vital capacity, and lowered levels of oxidative stress mediators by upregulating Nrf2 signaling in PF rats, similar to the results with Renshen Pingfei Decoction.

Ginsenosides have antiviral, anti-tumor, antioxidant and immunomodulatory pharmacological activities and are potential therapeutic agents for organ fibrosis disease [17–19]. Recent research has explored the role of ginseng in the treatment of fibrotic diseases. Guan et al [20] demonstrated an inhibitory effect of Rg1 on cigarette smoking-induced fibrosis. Rg1 inhibited the TGF-β1/Smad pathway in pulmonary fibroblasts *in vitro* and in a rat model of chronic obstructive pulmonary disease (COPD) *in vivo*. The dependence of the anti-fibrotic pharmacological action of Panax ginseng on ginsenoside content has been illustrated by many reports [21]. Ginsenosides may be divided into three groups based on chemical structure: protopanaxatriol (PPT), protopanaxadiol (PPD) and oleanane types [22], and are hydrolyzed in the gastrointestinal tract to form metabolites, including PPT and PPD, which are more easily absorbed [23] and have more potent activities than the original saponins [24–26]. Bioavailability of PPT and PPD have been estimated to be 3.69% and 48.12%, respectively, and PPT shown to be unstable in the stomach [27]. Therefore, the current study focused on PPD. Previous research on the effect of ginseng components on PF has focused on total ginsenosides [28] or ginsenoside Rg1 [29] with little work having been done on metabolites. A mouse model of PF induced by BLM was established, and the impact of PPD in relieving PF progression was examined. The aim was to illuminate the pathogenesis of PF and the anti-PF effect of protopanaxadiol.

2. Methods

2.1. Chemicals and reagents

PPD was supplied by Chengdu Biopurify Phytochemical Ltd. (Chengdu, China) and BLM and nintedanib (NDN) by Shanghai Yuanye Bio-Technology Co., Ltd. (Shanghai, China). All cell culture reagents came from Biosharp Technology Inc. (Hefei, China) and Gibco (Grand Island, NY, USA). Recombinant Mouse TGF-β1 was supplied by Suzhou Nearshore Protein Technology Co., Ltd. (Suzhou, China). PCR primers for TGF-β1, COL I, α-SMA, STING, E-cadherin, Vimentin and β-actin were purchased from Beijing Qingke Biological Technology Co., Ltd. (Beijing, China). Control small interfering RNA, STING-siRNA and AMPK-siRNA were provided by Santa Cruz Biotechnology Inc. (Dallas, Texas, U.S.A.). Antibodies raised against Smad2, p-Smad2, AMPK, p-AMPK and TGF-β1 were purchased from Affinity Biosciences LTD. (Ohio, USA) and against α-SMA, Col I, β-actin and GAPDH from Proteintech Group Inc. (Chicago, USA).

2.2. Animals

Seven-week-old male C57BL/6 mice weighing 20-22 g were purchased from the Comparative Medicine Centre of Yangzhou University (Yangzhou, China). Mice were acclimatized for 1 week in an air-conditioned room with a 12 h light/12 h dark cycle at a temperature of 22 °C ± 2 °C and humidity of 55 % ± 10 %. Care of animals followed the recommended protocols of the General Recommendation and Provisions of the Chinese Experimental Animals Administration Legislation, and ethical approval was obtained from the China Pharmaceutical University (CPU2020-05-008).

2.3. BLM-induced PF in mice

The establishment of the PF model was performed as described previously [30]. Mice were anesthetized by intraperitoneal injection of 50 mg·kg^{-1} 1% pentobarbital sodium and 3.5 mg·kg^{-1} BLM in 50 μL saline administered intratracheally using a tracheal cannula. One week after BLM administration, mice were randomly assigned to groups of equal numbers. PPD (saline suspension containing 0.5% CMC-Na sodium carboxymethylcellulose) was administered by an intragastric route for two consecutive weeks. Lung tissues were collected for pulmonary index measurements, histopathological examination, Western blotting and qRT-PCR analysis. The pulmonary index is used to give an approximate evaluation of pulmonary edema or fibrosis in experimental animals and distinguishes between heavier fibrotic lung tissue and lighter normal lung tissue by weight [31]. The pulmonary index formula is as follows:

$$\text{Pulmonary index (mg / g)} = \frac{\text{lung weight (mg)}}{\text{body weight (g)}}$$

2.4. Histopathology and immunohistochemistry analysis

Lung tissues were fixed, sliced and stained with Hematoxylin-Eosin (H&E) and Masson's trichrome for analysis of inflammation and lung collagen levels. Lung inflammation and fibrosis were assessed by an experienced pathologist, referring to a semi-quantitative histology score system [32,33]. STING expression was determined by immunohistochemistry (IHC). Fixed tissues were paraffin-embedded, incubated with anti-STING antibody (1:200), and five fields were randomly selected for evaluation of staining using an Olympus BX53 microscope at 200 × magnification.

2.5. Cell culture

Mouse alveolar epithelial cells (MLE-12, ZQ0470) were supplied by Zhong Qiao Xin Zhou Biotechnology Co., Ltd. (Shanghai, China) and cultured in Dulbecco's Modified Eagle Medium: Nutrient Mixture F-12 medium containing 10% fetal bovine serum, 100 units/mL penicillin and 10 mg·mL^{-1} streptomycin under a humidified 5% CO_2 atmosphere at 37 °C. MLE-12 cells between the 3rd and 5th passages were used, and media was changed every day until 80% confluency was reached

2.6. Immunofluorescence staining

MLE-12 cells were cultured in a 6-well cell culture plate, stimulated with TGF-β1, and treated with PPD 48 h later. Treated cells were incubated with 4% paraformaldehyde in PBS for 20 min and

with 0.2% Triton X-100 in PBS for 10 min. Cells were blocked with 5% horse serum and 2% BSA in PBS for 1 h, incubated with primary antibody specific for p-AMPK or STING (1:100) in 2% BSA in PBS at 4 °C overnight, and the next day Cy3 conjugated secondary antibody (1:200) was added in the dark for 1 h. DAPI was used to stain nuclei for 12 min, and image analysis was performed by fluorescence microscopy (Olympus IX53).

2.7. Co-immunoprecipitation

MLE-12 cells were re-suspended in RIPA buffer plus protease inhibitor cocktail and lysed on ice for 15 min. Lysate supernatants were collected, and an aliquot was added to sample buffer. Target antibody or IgG was added to remaining samples and incubated overnight at 4 °C. 20 μL protein A + G agarose was added to samples and incubated at 4 °C for 4-6 h. Samples were washed with PBS, an equal volume of loading buffer was added, and Western blotting was performed.

2.8. Cellular thermal shift assay

MLE-12 cells were cultured in 100mm diameter dishes, prepared as described previously [34], and 7 samples of 100 μL each were taken from each group. Samples were incubated at 37, 42, 47, 52, 57, 62 and 67 °C for 3 min and then put into cold storage. Samples were centrifuged at 12000 g at 4 °C for 10 min, supernatants were added to the loading buffer, and Western blotting was performed.

2.9. siRNA transfection

MLE-12 cells were cultured on 6-well cell culture plates and transfected with 1 pmol small interfering RNA (siRNA) -control, siRNA STING or siRNA AMPK using Lipofectamine™3000 Reagent (Invitrogen, USA), according to the manufacturer's instructions. Cells were stimulated with TGF-β1 and treated with PPD for 48 h before further analysis.

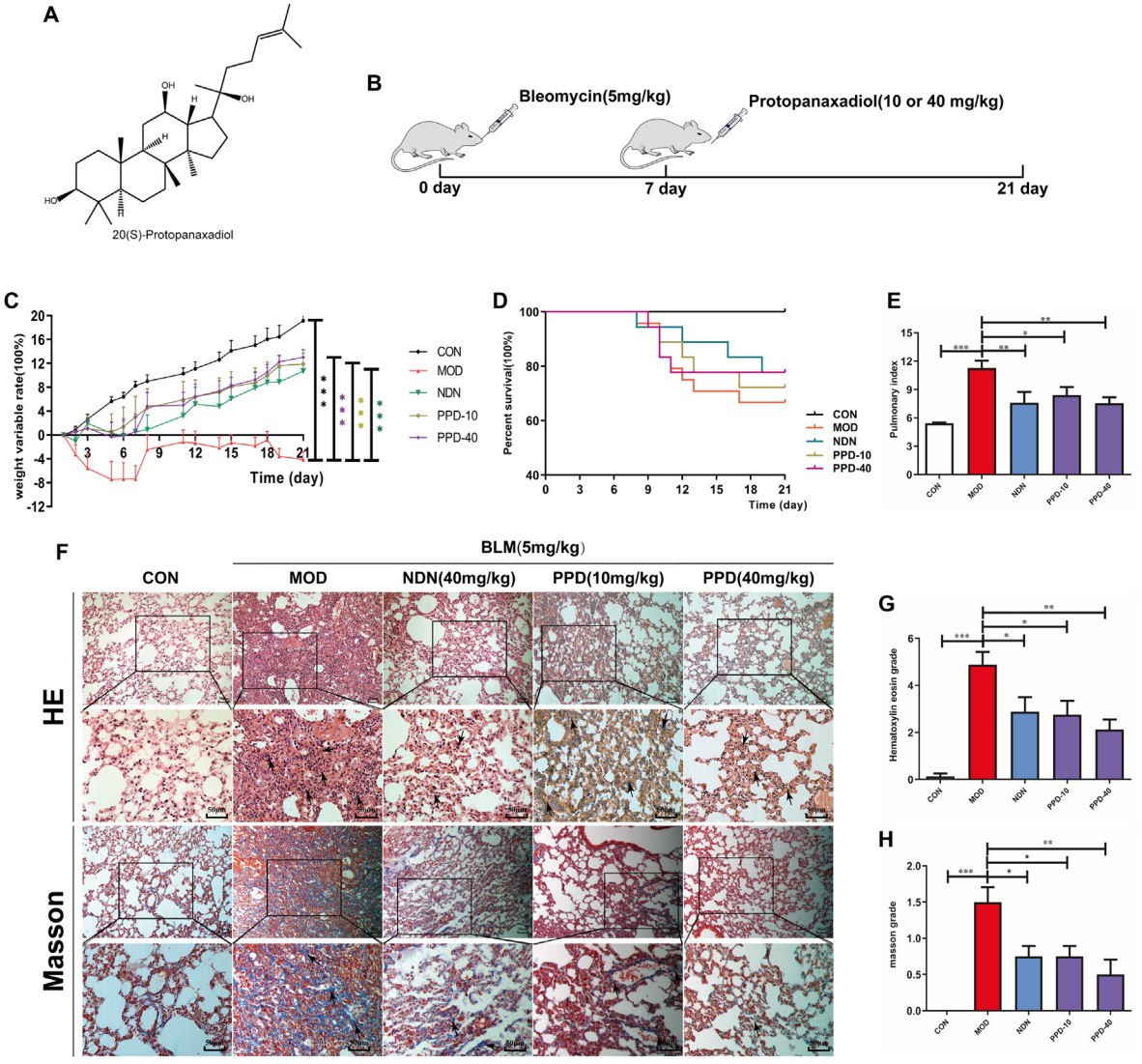

Fig. 1. Effects of PPD on BLM-induced pulmonary fibrosis in mice. (A) Chemical structure of PPD. (B) Schematic of the experimental effect of PPD on BLM-induced PF in mice. Mice were sacrificed, and lung tissue was taken on day 21 after intratracheal administration of 3.5 mg/kg BLM. Intragastric PPD (10 or 40 mg/kg) or NDN (40 mg/kg, positive drug) was given for 14 consecutive days after 7 days of intratracheal BLM administration. (C) Mouse weights during the experimental period. (D) Percent survival. (E) Pulmonary index. (F) Representative pathological lung sections (H&E and Masson's staining), scale bar = 50 μm. (G&H) Lung inflammation and fibrosis scores. Means ± S.D. are presented (n = 9). *$p < 0.05$, **$p < 0.01$, ***$p < 0.001$. PPD: protopanaxadiol. NDN: nintedanib.

2.10. Total RNA isolation and qRT-PCR analysis

Total RNA was extracted from cells and tissues using RNA-Quick Purification Kit (YiShan Biotech, Shanghai, China), reverse transcribed with HiScript® II Q RT SuperMix kit (Vazyme Biotech Co., Ltd, Nanjing, China) and qRT-PCR performed using ChamQ™ SYBR® qPCR Master Mix (Low ROX Premixed) kit (Vazyme Biotech Co., Ltd, Nanjing, China). β-actin was used as reference gene, and data were analyzed using the ΔΔCt method. Primer sequences are listed in Supplementary Table 1.

2.11. Western blotting

Cells and tissue samples were lysed using RIPA buffer (ELPIS Biotech Inc., Dae-jeon, Korea), proteins separated by 10% SDS-PAGE, transferred to a PVDF membrane and incubated at 4 °C with primary antibodies overnight and with secondary antibodies for 1 h. Membranes were developed using enhanced chemiluminescence (ECL) detection kit (Vazyme Biotech Co., Ltd, Nanjing, China).

2.12. Statistical analysis

All data are presented as mean ± S.D. Survival curves were analyzed using Kaplan-Meier. Statistical comparisons were made using one-way ANOVA with Tukey's multiple comparison test and two-way ANOVA with Bonferroni's post-hoc testing. A value of $p < 0.05$ was considered to indicate statistical significance.

3. Results

3.1. PPD had a therapeutic effect on PF induced by BLM.

PPD is a tetracyclic triterpenoid found in ginseng (Fig. 1A). Mice with acute PF induced by BLM (Fig. 1B) showed significant weight loss and reduced food and water intake. No other symptoms, such as diarrhea, were present apart from a certain degree of dyspnea. PPD improved weight (Fig. 1C) and reduced the pulmonary index of mice with PF (Fig. 1E). Continuous intragastric administration of 10 or 40 $mg \cdot kg^{-1} \cdot day^{-1}$ PPD for 14 d improved BLM-induced PF and reduced inflammation and collagen deposition in lung tissue (Fig. 1F–H).

3.2. PPD regulated some classical indicators and pathways in PF mice.

TGF-β1 mRNA and phosphorylated Smad2 protein expression were up-regulated in PF model lung tissue relative to controls (Fig.2A-C). COL I and α-SMA protein and mRNA levels all increased

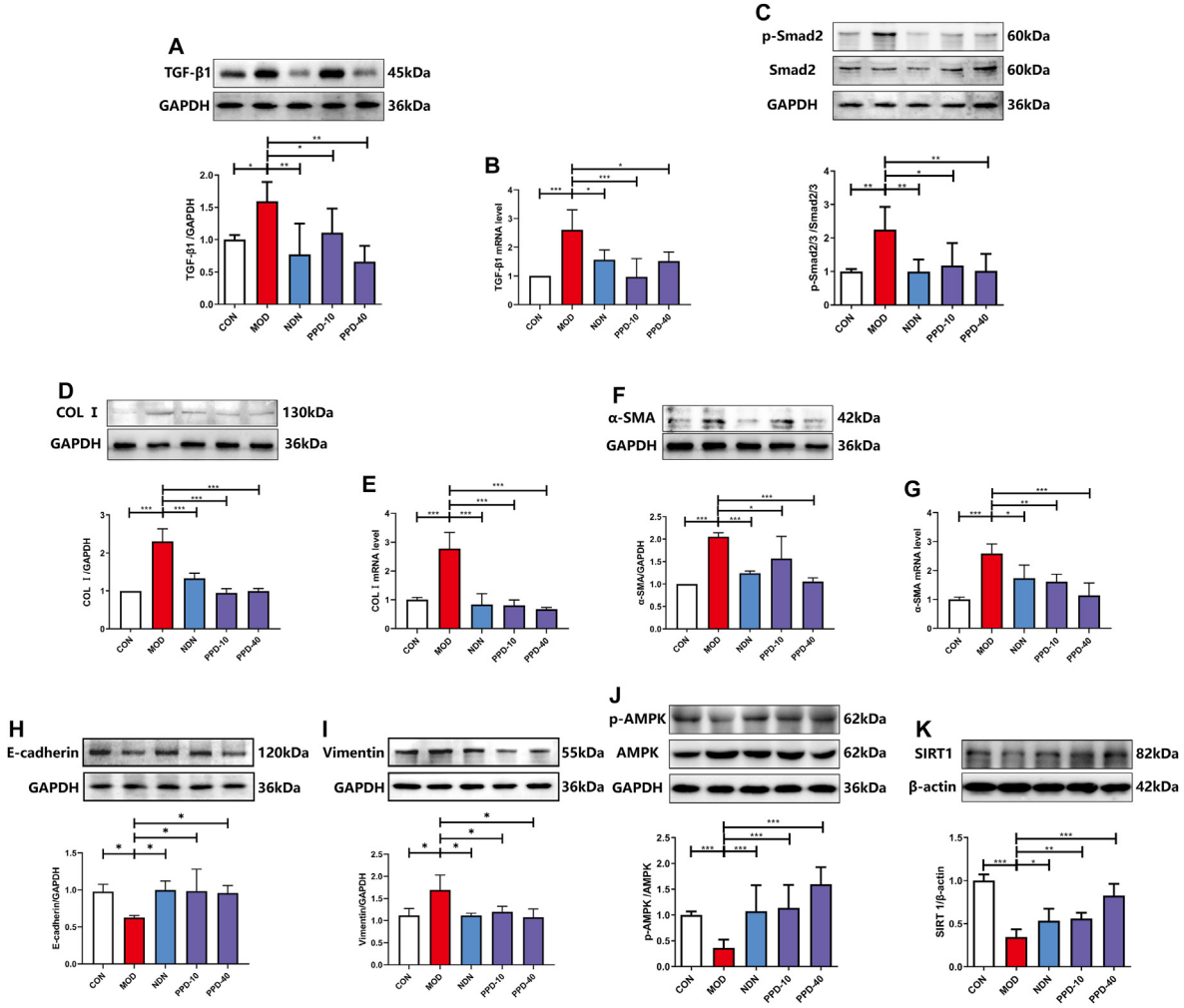

Fig. 2. The effect of PPD on TGF-β1 and AMPK signaling pathways in lung tissue of mice with BLM-induced pulmonary fibrosis. (A&B) TGF-β1 protein and mRNA levels. (C) p-Smad2 protein expression. (D-G) Col I and α-SMA protein and mRNA levels. (H–K) E-cadherin, Vimentin, p-AMPK and SIRT1 protein expression. Protein was detected in lung tissues by Western blotting and mRNA levels by qRT-PCR, and data are shown as mean ± S.D. (n = 4). *$p < 0.05$, **$p < 0.01$, ***$p < 0.001$.

(Fig.2D-G). Administration of 10 or 40 mg·kg^{-1} PPD down-regulated TGF-β1, p-Smad2, COL I and α-SMA protein expression. PPD has been suggested to inhibit the TGF-β1/Smad2 signaling pathway and relieve BLM-induced collagen deposition in lung tissue. PPD also restored abnormal E-cadherin and Vimentin expression in lung tissue caused by BLM, suggesting a favorable impact on the epithelial-mesenchymal transition (Fig.2H&I). In addition, PPD promoted AMPK activation and down-regulated SIRT1 protein expression, suggesting a regulatory effect on energy metabolism (Fig.2J&K).

3.3. PPD regulated STING protein expression and AMPK phosphorylation.

Intragastric administration of 10 or 40 mg·kg^{-1} PPD reduced the expression of STING protein, which has been shown to be involved in tissue fibrosis, compared with untreated PF mice ($p < 0.01$, Fig.3A). On days 14 and 21 after BLM induction, STING was highly expressed in the lung tissue of PF mice and AMPK phosphorylation was inhibited (Fig.3B). Increased STING expression and AMPK inactivation correlated positively with the degree of inflammation and fibrosis ($p < 0.01$, Fig. 3C–J). In summary, PPD regulated STING protein expression and AMPK phosphorylation after 7 d of

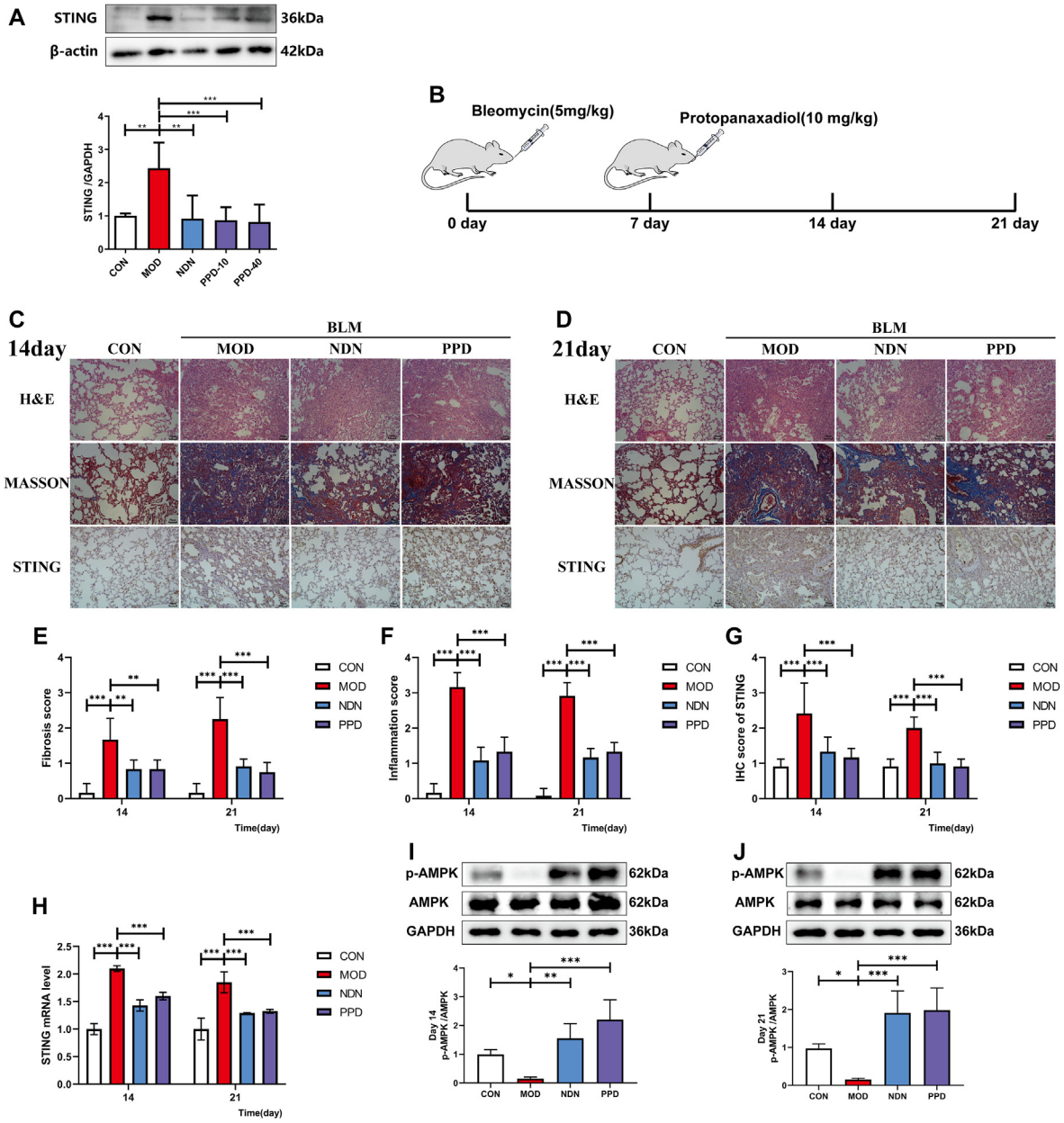

Fig. 3. Regulation of STING by PPD during bleomycin-induced lung fibrogenesis in mice. (A) Lung STING expression by Western blotting. (B) Scheme showing regulation of STING levels by PPD from BLM-induced mice. Mice were sacrificed for lung tissue sampling on days 14 and 21 after intratracheal administration with 3.5 mg/kg BLM. Intragastric PPD (40 mg/kg) or NDN (40 mg/kg, positive drug) was given for 14 consecutive days after 7 days of intratracheal BLM administration. (C-D) Representative micrographs of H&E, Masson's staining and STING immunohistochemistry in lung pathological sections at days 14 and 21 after intratracheal BLM administration, scale bar = 50 μm. (E&F) Lung inflammation and fibrosis scores at days 14 and 21 after intratracheal BLM administration. (G) Lung immunohistochemical scores; (H) STING mRNA in lung tissue at days 14 and 21 after intratracheal BLM administration by qRT-PCR. (I&J) AMPK and p-AMPK expression in lung at days 14 and 21 after intratracheal BLM administration by Western blotting. Data are expressed as mean ± S.D. (n = 4). *$p < 0.05$, **$p < 0.01$, ***$p < 0.001$.

continuous administration, exerting anti-fibrotic effects comparable to the drug NDN.

3.4. PPD treated PF by activating AMPK

PPD had no significant cytotoxicity on the alveolar epithelial cell-line, MLE-12 at a concentration of 2 μM (Fig. 4A). PPD inhibited the epithelial-mesenchymal transition of MLE-12 induced by TGF-β1, increased E-cadherin and down-regulated vimentin expression (Fig. 4B&C). CETSA-Wes and molecular docking experiments showed that PPD may bind AMPK to promote its activation (Fig. 4D–F). Immunofluorescence results showed that PPD regulated expression of p-AMPK and STING in MLE-12 cells induced by TGF-β1 (Fig. 4G&H).

3.5. PPD inhibited STING expression by activating AMPK

MLE-12 cells treated with TGF-β1 were transfected with siRNAs. Transfection with siRNA-AMPK affected PPD regulation of E-cadherin and vimentin mRNA and protein levels (Fig. 5A–D). In addition, siRNA-AMPK transfection also blocked the inhibition of STING mRNA and protein expression by PPD (Fig. 5E&F). AMPK activation was shown to inhibit expression of STING protein by co-immunoprecipitation experiments (Fig. 5G). Transfection with siRNA-STING did not change the effect of PPD on expression of E-cadherin and vimentin mRNA or protein (Fig. 5H–K), nor did it affect AMPK activation (Fig. 5L). Thus, PPD may inhibit STING expression by activating AMPK to regulate the immune function of the body.

3.6. PPD exerted anti-PF effects by regulating AMPK/STING.

The AMPK activator, metformin, was used as a positive control to observe differences before and after combined administration of PPD and the AMPK inhibitor, Compound C (Fig. 6A). The STING inhibitor, C-176, was used as a positive control to observe differences before and after the combined administration of PPD and STING activator, CMA. PPD exerted a similar effect to that of metformin, and combined administration of Compound C blocked the anti-fibrotic effect of PPD on lung tissue. Similarly, C-176 improved BLM-induced weight loss, inflammation and fibrosis of lung tissue and combined administration of STING activator, CMA, also blocked

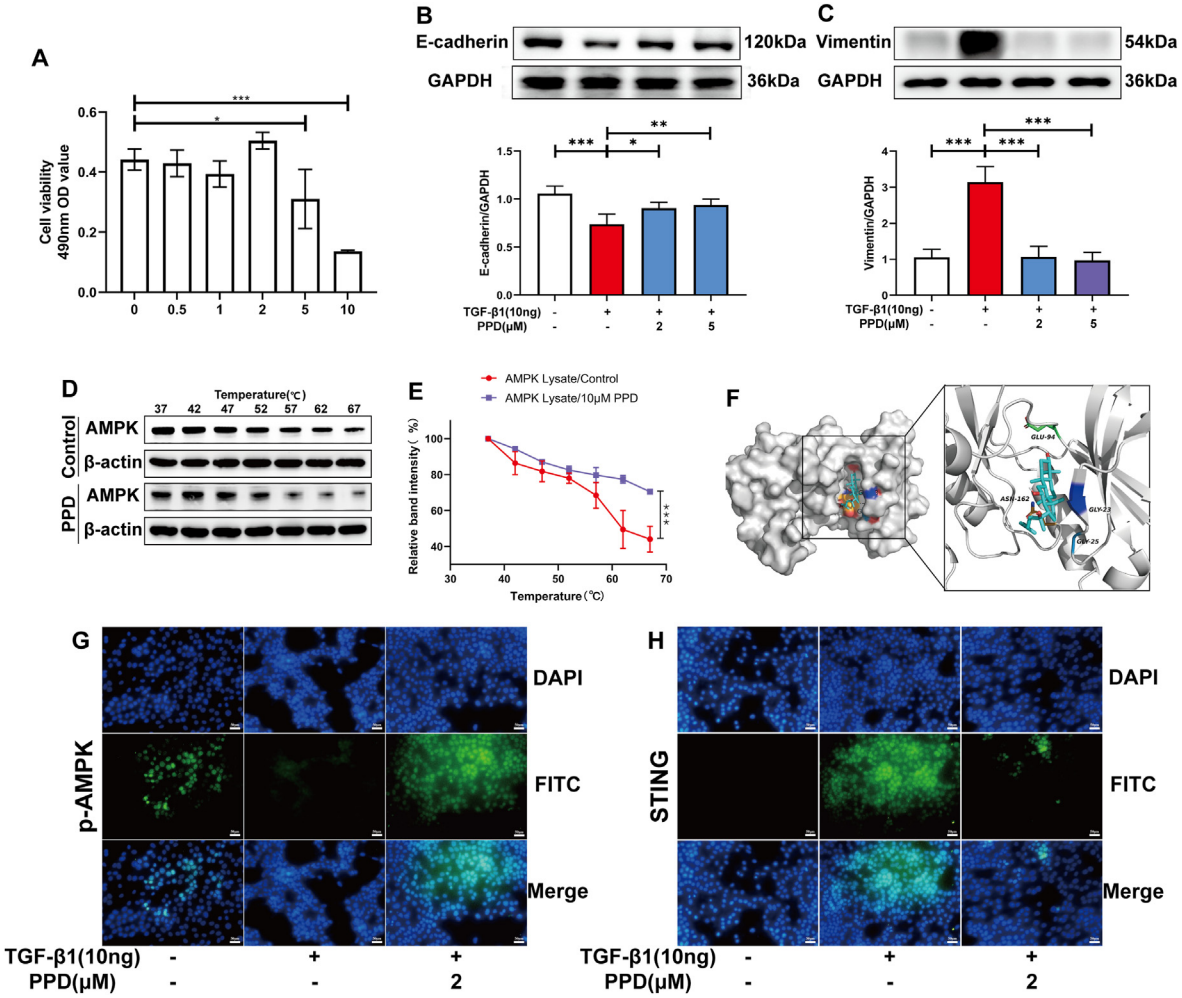

Fig. 4. The role of AMPK during PPD regulation of TGF-β1-treated MLE-12 cells. MLE-12 cells were treated with 10 ng/ml TGF-β1 or protopanaxadiol for 48 h. (A) PPD cytotoxicity (0-10 μM) towards MLE-12 was determined using an MTT assay. (B&C) E-cadherin and Vimentin proteins were detected by Western blotting. (D&E) CETSA-Wes investigation of AMPK-PPD interactions. (F) Molecular docking images of protopanaxadiol with AMPK. (G&H) p-AMPK and STING protein detected by immunofluorescence. Data are presented as mean ± S.D. (n = 4). *$p < 0.05$, **$p < 0.01$, ***$p < 0.001$.

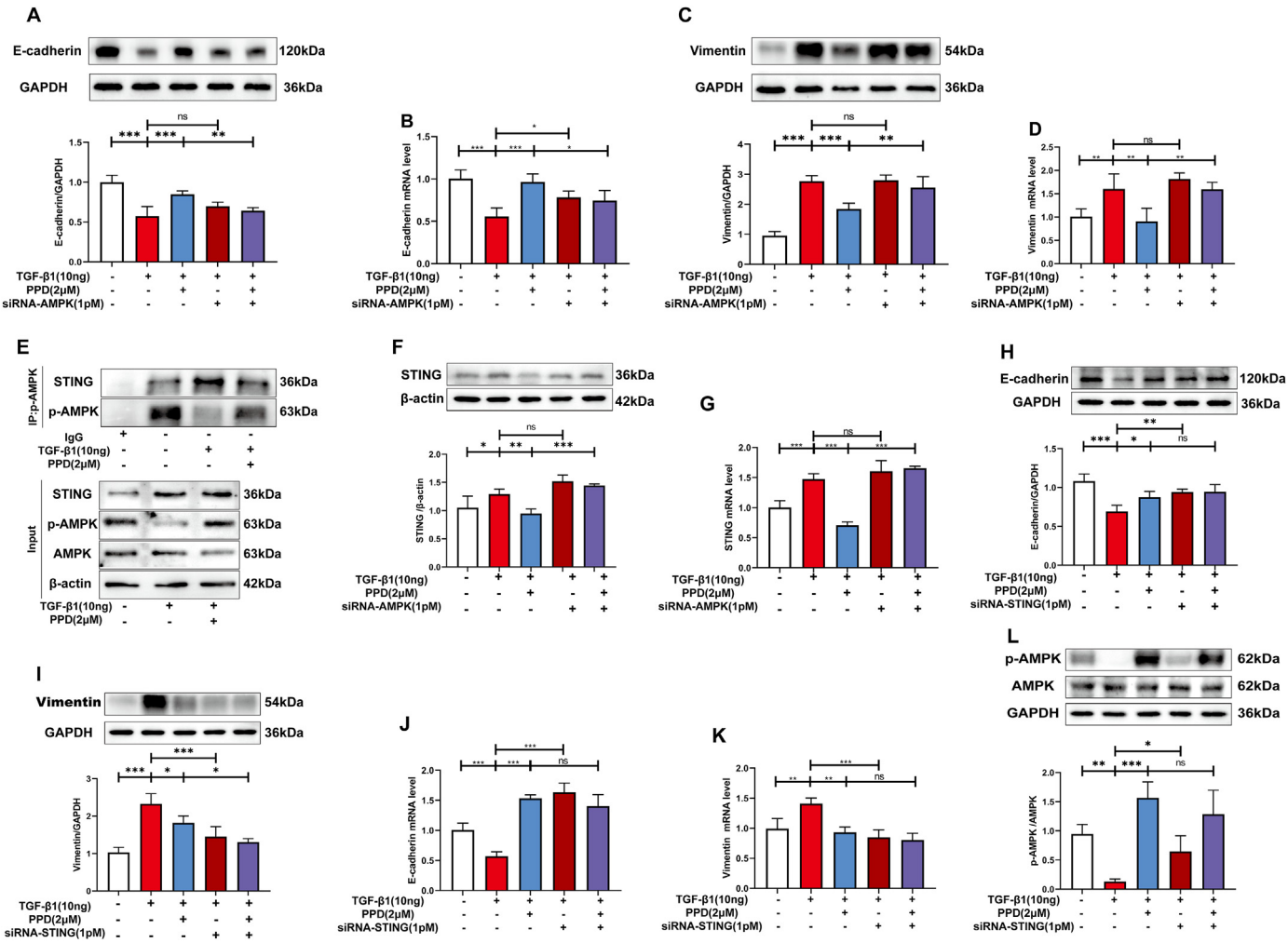

Fig. 5. AMPK activation and STING involvement in the antifibrotic effects of PPD in TGF-β1-treated MLE-12 cells. (A-D) MLE-12 cells were transfected with AMPK-siRNA, and expression of E-cadherin and Vimentin protein was detected by Western blotting. E-cadherin and Vimentin mRNA were detected by qRT-PCR. (E&F) MLE-12 cells were transfected with siRNA-AMPK, and STING mRNA and protein levels were determined. (G) p-AMPK binding to STING in MLE-12 cells exposed to TGF-β1. (H-L) MLE-12 were transfected with siRNA-STING and E-cadherin, Vimentin and p-AMPK protein detected by Western blotting. E-cadherin and Vimentin mRNA were detected by qRT-PCR. Data are presented as mean ± S.D. (n = 4). $*p < 0.05$, $**p < 0.01$, $***p < 0.001$.

the anti-fibrosis effect of PPD. In addition, combined administration of Compound C blocked the inhibitory effect of PPD on STING mRNA production. In conclusion, PPD exerts an anti-PF effect by activating AMPK and inhibiting STING expression.

4. Discussion

The current data have demonstrated that PPD caused phosphorylation and activation of AMPK to regulate STING expression and also regulated AMPK/SIRT1 and TGF-β1/Smad2 signaling. Numerous cytokines and chemokines involved in the adaptive immune response were produced and protected against lung injury, had anti-oxidant, free radical-scavenging effects, and regulated MMP expression [35–37]. PPD is produced after ginsenosides have activated the hypoglycemic metabolism of gastrointestinal flora and ameliorated PF via multiple targets and pathways.

STING expression changed with the degree of inflammation in PF. STING is an endoplasmic reticulum receptor able to induce innate immune responses appropriate to the microenvironment and cell type and to regulate immunotherapy and autoimmunity [38–41]. PPD may reduce BLM-induced PF by inducing autophagy and inhibiting cell death under conditions of endoplasmic reticulum stress [42]. However, PPD did not directly suppress STING expression but required activated AMPK to bring about this effect. AMPK knockout affected PPD inhibition of STING, but STING knockout did not affect PPD activation of AMPK or its therapeutic effect on PF. High STING expression may also inhibit AMPK phosphorylation, aggravating PF. However, the connection between STING and AMPK is unclear. The current data demonstrate that AMPK activation or STING inhibition had therapeutic effects on PF similar to those of PPD. STING activation aggravated PF, demonstrating antagonism of PPD.

PPD alleviated PF, and CESTA experiments showed AMPK to be a target protein which was shown to act on STING by co-immunoprecipitation and transfection of small interfering RNA. However, the question of how changes in STING improve PF requires further in-depth study. PPD may be able to regulate mitochondrial energy metabolism through AMPK, inhibiting the accumulation of reactive oxygen species to treat oxidative damage, and may also be able to regulate intestinal flora. The impact of PPD

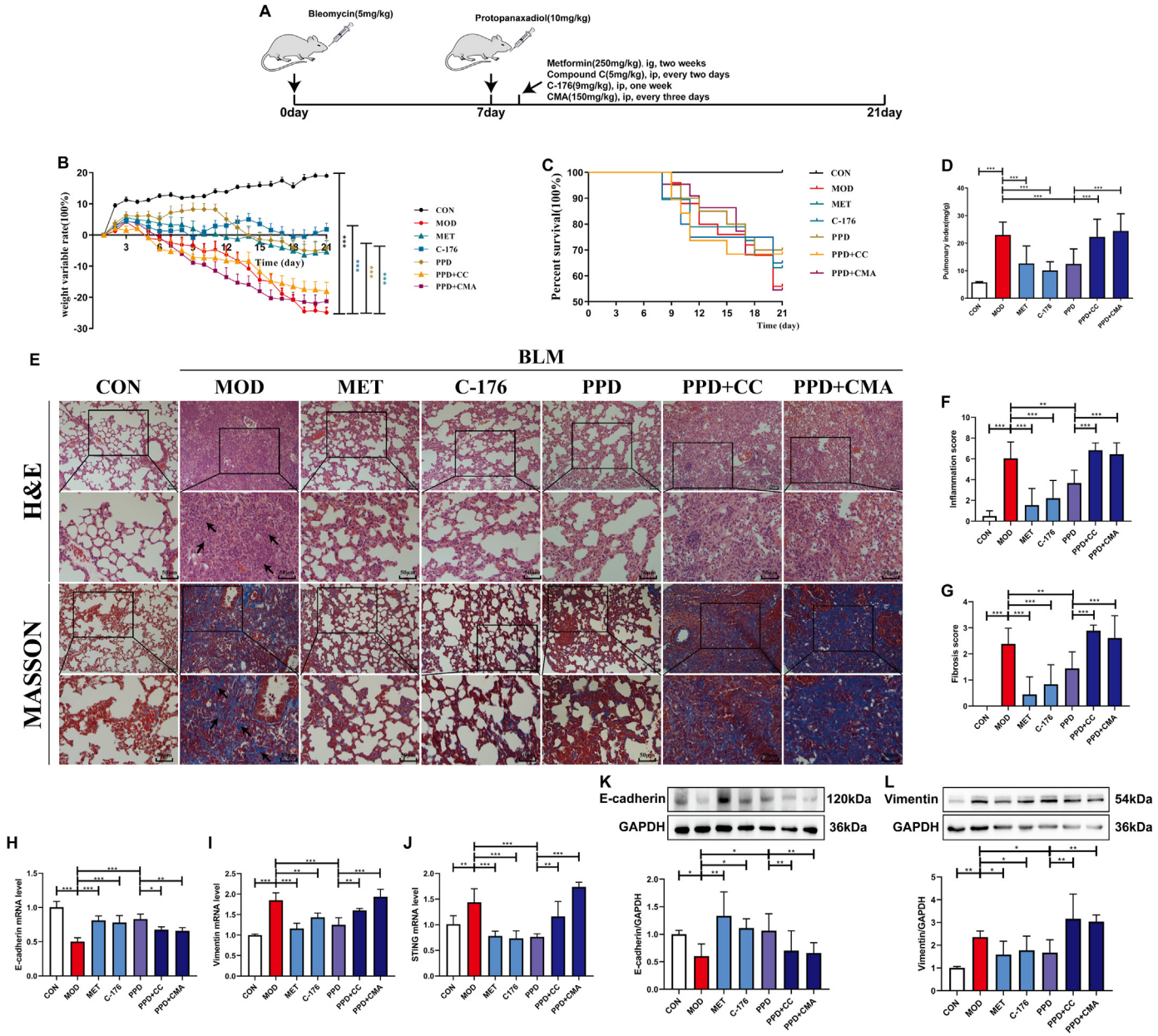

Fig. 6. Key roles for AMPK activation and STING inhibition in the anti-PF effect of PPD. (A) Experimental scheme showing co-treatment of BLM-induced PF mice with 40 mg/kg PPD and 5 mg/kg Compound C (AMPK inhibitor) or 150 mg/kg CMA (STING inhibitor). Metformin (250 mg/kg) and C-176 (9 mg/kg) were used as positive drugs. (B) Weight changes during the experimental period. (C) Percent survival. (D) Pulmonary index. (E) Representative lung pathological sections (H&E and Masson's staining), scale bar = 50 μm. (F&G) Lung inflammation and fibrosis scores. (H-J) E-cadherin, Vimentin, and STING mRNA were detected by qRT-PCR. (K&L) E-cadherin and Vimentin proteins were detected by Western blotting (n = 4). Data are expressed as mean ± S.D. (n = 9). *p < 0.05, **p < 0.01, ***p < 0.001.

on energy metabolism and immunity indicate its potential for use as an adjuvant drug for the clinical treatment of PF. Further experiments to clarify specific mechanisms are required.

In summary, PPD may prove to be a promising treatment for human PF through its immunomodulatory effects and action on AMPK.

Authors' contributions

Guoqing Ren, Weichao Lv and Yue Ding performed the experiments. Guoqing Ren and Lei Wang wrote the manuscript. Zheng-Guo Cui, Renshi Li provided experimental guidance. Jiangwei Tian and Chaofeng Zhang designed and rationalized the project. All authors reviewed and approved the manuscript.

Funding

This work was supported by grants from the National Natural Science Foundation of China (81773982 for Chaofeng Zhang; 21775166 for Jiangwei Tian; 82003937 for Renshi Li), and Youth Academic leaders of the Qinglan Project in Jiangsu province (to Chaofeng Zhang).

Declaration of competing interest

The authors declare no conflict of interest, financial or otherwise.

Acknowledgments

We are thankful to all the authors for their dedication and patience throughout the study. The authors would like to express their gratitude to EditSprings (https://www.editsprings.com/) for the expert linguistic services provided.

Appendix A. Supplementary data

Supplementary data to this article can be found online at https://doi.org/10.1016/j.jgr.2023.01.002.

References

[1] Pardo A, Selman M. Lung fibroblasts, aging, and idiopathic pulmonary fibrosis. Ann Am Thorac Soc 2016:S417–21. https://doi.org/10.1513/AnnalsATS.201605-341AW.
[2] Moss BJ, Ryter SW, Rosas IO. Pathogenic mechanisms underlying idiopathic pulmonary fibrosis. Annu Rev Pathol 2021. https://doi.org/10.1146/effectonannurev-pathol-042320-030240.
[3] Tao N, Li K, Liu J, Fan G, Sun T. Liproxstatin-1 alleviates bleomycin-induced alveolar epithelial cells injury and mice pulmonary fibrosis via attenuating inflammation, reshaping redox equilibrium, and suppressing ROS/p53/α-SMA pathway. Biochem Biophys Res Commun 2021;551:133–9. https://doi.org/10.1016/j.bbrc.2021.02.127.
[4] Li X, Liu X, Deng R, Gao S, Yu H, Huang K, et al. Nintedanib inhibits wnt3a-induced myofibroblast activation by suppressing the Src/β-catenin pathway. Front Pharmacol 2020;11:310. https://doi.org/10.3389/fphar.2020.00310.
[5] Liu J, Peng D, You J, Zhou O, Qiu H, Hao C, et al. Type 2 alveolar epithelial cells differentiated from human umbilical cord mesenchymal Stem cells alleviate mouse pulmonary fibrosis through β-catenin-regulated cell apoptosis. Stem Cells Dev 2021;30(13):660–70. https://doi.org/10.1089/scd.2020.0208.
[6] Mora AL, Bueno M, Rojas M. Mitochondria in the spotlight of aging and idiopathic pulmonary fibrosis. J Clin Invest 2017;127(2):405–14. https://doi.org/10.1172/JCI87440.
[7] Zhang H, Davies KJA, Forman HJ. Oxidative stress response and Nrf2 signaling in aging. Free Radic Biol Med 2015;88:314–36. https://doi.org/10.1016/j.freeradbiomed.2015.05.036.
[8] Bargagli E, Olivieri C, Bennett D, Prasse A, Muller-Quernheim J, Rottoli P. Oxidative stress in the pathogenesis of diffuse lung diseases: a review. Respir Med 2009;103(9):1245–56. https://doi.org/10.1016/j.rmed.2009.04.014.
[9] Nishio T, Koyama Y, Liu X, Rosenthal SB, Yamamoto G, Fuji H, et al. Immunotherapy-based targeting of MSLN activated portal fibroblasts is a strategy for treatment of cholestatic liver fibrosis. Proc Natl Acad Sci U S A 2021;(29):118. https://doi.org/10.1073/pnas.2101270118.
[10] Tian M, Liu W, Zhang Q, Huang Y, Li W, Wang W, et al. MYSM1 represses innate immunity and autoimmunity through suppressing the cGAS-STING pathway. Cell Rep 2020;33(3):108297. https://doi.org/10.1016/j.celrep.2020.108297.
[11] Dobbs N, Burnaevskiy N, Chen D, Gonugunta VK, Alto NM, Yan N. STING activation by translocation from the ER is associated with infection and autoinflammatory disease. Cell Host Microbe 2015;18(2):157–68. https://doi.org/10.1016/j.chom.2015.07.001.
[12] Savigny F, Schricke C, Lacerda-Queiroz N, Meda M, Nascimento M, Huot-Marchand S, et al. Protective role of the nucleic acid Sensor STING in pulmonary fibrosis. Front Immunol 2020;11:588799. https://doi.org/10.3389/fimmu.2020.588799.
[13] Han B, Wang X, Wu P, Jiang H, Yang Q, Li S, et al. Pulmonary inflammatory and fibrogenic response induced by graphitized multi-walled carbon nanotube involved in cGAS-STING signaling pathway. J Hazard Mater 2021;417:125984. https://doi.org/10.1016/j.jhazmat.2021.125984.
[14] Jang SS, Kim HG, Han JM, Lee JS, Choi MK, Huh GJ, et al. Modulation of radiation-induced alterations in oxidative stress and cytokine expression in lung tissue by Panax ginseng extract. Phytother Res 2015;29(2):201–9. https://doi.org/10.1002/ptr.5223.
[15] Chen F, Wang PL, Fan XS, Yu JH, Zhu Y, Zhu ZH. Effect of Renshen Pingfei Decoction, a traditional Chinese prescription, on IPF induced by Bleomycin in rats and regulation of TGF-β1/Smad3. J Ethnopharmacol 2016;186:289–97. https://doi.org/10.1016/j.jep.2016.03.051.
[16] Bai Y, Li J, Zhao P, Li Y, Li M, Feng S, et al. A Chinese herbal formula ameliorates pulmonary fibrosis by inhibiting oxidative stress via upregulating Nrf2. Front Pharmacol 2018;9:628. https://doi.org/10.3389/fphar.2018.00628.
[17] Deng J, Lv XT, Wu Q, Huang XN. Ginsenoside Rg (1) inhibits rat left ventricular hypertrophy induced by abdominal aorta coarctation: involvement of calcineurin and mitogen-activated protein kinase signalings. Eur J Pharmacol 2009;608:42–7. https://doi.org/10.1016/j.ejphar.2009.01.048.
[18] Yu XF, Deng J, Yang DL, Gao Y, Gong QH, Huang XN. Total Ginsenosides suppress the neointimal hyperplasia of rat carotid artery induced by balloon injury. Vascul Pharmacol 2011;54:52–7. https://doi.org/10.1016/j.vph.2010.12.003.
[19] Liu H, Lv C, Lu J. Panax ginseng C. A. Meyer as a potential therapeutic agent for organ fibrosis disease. Chin Med 2020;15(1):124. https://doi.org/10.1186/s13020-020-00400-3.
[20] Guan S, Liu Q, Han F, Gu W, Song L, Zhang Y, Guo X, Xu W. Ginsenoside Rg1 ameliorates cigarette smoke-induced airway fibrosis by suppressing the TGF-beta1/Smad pathway in vivo and in vitro. Biomed Res Int 2017;2017:6510198.
[21] Li X, Mo N, Li ZZ. Ginsenosides: potential therapeutic source for fibrosis-associated human diseases. J Ginseng Res 2020;44(3):386–98. https://doi.org/10.1016/j.jgr.2019.12.003.
[22] Choi KT. Botanical characteristics, pharmacological effects and medicinal components of Korean Panax ginseng C A Meyer. Acta Pharmacol Sin 2008;29:1109–18. https://doi.org/10.1111/j.1745-7254.2008.00869.x.
[23] Hasegawa H, Sung JH, Benno Y. Role of human intestinal Prevotella oris in hydrolyzing ginseng saponins. Planta Med 1997;63:436–40. https://doi.org/10.1055/s-2006-957729.
[24] Hasegawa H. Proof of the mysterious efficacy of ginseng: basic and clinical trials: metabolic activation of ginsenoside: deglycosylation by intestinal bacteria and esterification with fatty acid. J Pharmacol Sci 2004;95:153–7. https://doi.org/10.1254/jphs.fmj04001x4.
[25] Sun L, Wang Q, Liu X, Brons NH, Wang N, Steinmetz A, et al. Anti-cancer effects of 20(S)-protopanoxadiol on human acute lymphoblastic leukemia cell lines Reh and RS4;11. Med Oncol 2011;28:813–21. https://doi.org/10.1007/s12032-010-9508-1.
[26] Chen G, Yang M, Nong S, Yang X, Ling Y, Wang D, et al. Microbial transformation of 20(S)-protopanaxadiol by Absidia corymbifera. Cytotoxic activity of the metabolites against human prostate cancer cells. Fitoterapia 2013;84:6–10. https://doi.org/10.1016/j.fitote.2012.09.018.
[27] Kong LT, Wang Q, Xiao BX, Liao YH, He XX, Ye LH, et al. Different pharmacokinetics of the two structurally similar dammarane sapogenins, protopanaxatriol and protopanaxadiol, in rats. Fitoterapia 2013;86:48–53. https://doi.org/10.1016/j.fitote.2013.01.019.
[28] Yang L, Chen PP, Luo M, Shi WL, Hou DS, Gao Y, et al. Inhibitory effects of total ginsenoside on bleomycin-induced pulmonary fibrosis in mice. Biomed Pharmacother 2019;114:108851. https://doi.org/10.1016/j.biopha.2019.108851.
[29] Zhan H, Huang F, Ma W, Zhao Z, Zhang H, Zhang C. Protective effect of ginsenoside Rg1 on bleomycin-induced pulmonary fibrosis in rats: involvement of caveolin-1 and TGF-beta1 signal pathway. Biol Pharm Bull 2016;39:1284e92. https://doi.org/10.1248/bpb.b16-00046.
[30] Tao L, Yang J, Cao F, Xie H, Zhang M, Gong Y, et al. Mogroside IIIE, a novel anti-fibrotic compound, reduces pulmonary fibrosis through Toll like receptor 4 pathways. J Pharmacol Exp Ther 2017;361(2):268–79. https://doi.org/10.1124/jpet.116.239137.
[31] Yang JY, Tao LJ, Liu B, You XY, Zhang CF, Xie HF, Li RS. Wedelolactone attenuates pulmonary fibrosis partly through activating AMPK and regulating raf-MAPKs signaling pathway. Front Pharmacol 2019;10:151. https://doi.org/10.3389/fphar.2019.00151.
[32] Szapiel SV, Elson NA, Fulmer JD, Hunninghake GW, Crystal RG. Bleomycin-induced interstitial pulmonary disease in the nude, athymic mouse. Am Rev Respir Dis 1979;120(4):893–9. https://doi.org/10.1164/arrd.1979.120.4.893.
[33] Seger S, Stritt M, Vezzali E, Nayler O, Hess P, Groenen PMA, et al. A fully automated image analysis method to quantify lung fibrosis in the bleomycin-induced rat model. PLoS One 2018;13(3):e0193057. https://doi.org/10.1371/journal.pone.0193057.
[34] Jafari R, Almqvist H, Axelsson H, Ignatushchenko M, Lundbäck T, Nordlund P, Martinez MD. The cellular thermal shift assay for evaluating drug target interactions in cells. Nat Protoc 2014;9(9):2100–22. https://doi.org/10.1038/nprot.2014.138.
[35] Qin N, Yang W, Feng D, Wang X, Qi M, Du T, et al. Total ginsenosides suppress monocrotaline-induced pulmonary hypertension in rats: involvement of nitric oxide and mitogen-activated protein kinase pathways. J Ginseng Res 2016;40(3):285–91. https://doi.org/10.1016/j.jgr.2015.09.005.
[36] Aa JY, Wang GJ, Hao HP, Huang Q, Lu YH, Yan B, et al. Differential regulations of blood pressure and perturbed metabolism by total ginsenosides and conventional antihypertensive agents in spontaneously hypertensive rats. Acta Pharmacol Sin 2010;31(8):930–7. https://doi.org/10.1038/aps.2010.86.
[37] Hafez MM, Hamed SS, El-Khadragy MF, Hassan ZK, Al Rejaie SS, Sayed-Ahmed MM, et al. Effect of ginseng extract on the TGF-β1 signaling pathway in CCl-induced liver fibrosis in rats. BMC Complement Altern Med 2017;17(1):45. https://doi.org/10.1186/s12906-016-1507-0.
[38] Ishikawa H, Barber GN. STING is an endoplasmic reticulum adaptor that facilitates innate immune signalling. Nature 2008;455(7213):674–8. https://doi.org/10.1038/nature07317.
[39] Iurescia S, Fioretti D, Rinaldi M. Targeting cytosolic nucleic acid-sensing pathways for cancer immunotherapies. Front Immunol 2018;9:711. https://doi.org/10.3389/fimmu.2018.00711.
[40] Wu JJ, Zhao L, Hu HG, Li WH, Li YM. Agonists and inhibitors of the STING pathway: potential agents for immunotherapy. Med Res Rev 2020;40(3):1117–41. https://doi.org/10.1002/med.21649.
[41] Paludan SR, Bowie AG. Immune sensing of DNA. Immunity 2013;38(5):870–80. https://doi.org/10.1016/j.immuni.2013.05.004.
[42] Baek AR, Hong J, Song KS, Jang AS, Kim DJ, Chin SS, et al. Spermidine attenuates bleomycin-induced lung fibrosis by inducing autophagy and inhibiting endoplasmic reticulum stress (ERS)-induced cell death in mice. Exp Mol Med 2020;52(12):2034–45. https://doi.org/10.1038/s12276-020-00545-z.